

# Raman spectra of a two-dimensional electron gas in narrow-gap semiconductor quantum wells in magnetic fields: Spin-flip and anisotropic effects

V. López-Richard and G.-Q. Hai

*Instituto de Física de São Carlos, Universidade de São Paulo, 13560-970, São Carlos, SP, Brazil*

C. Trallero-Giner

*Department of Theoretical Physics, Havana University, San Lazaro y L, 10400 Havana, Cuba*

G. E. Marques

*Departamento de Física, Universidade Federal de São Carlos, 13565-905, São Carlos, SP, Brazil*

(Received 8 January 2002; revised manuscript received 12 April 2002; published 2 October 2002)

The effects of the interband coupling on the magnetoplasmons and the single-particle excitations are studied for a two-dimensional electron gas in narrow-gap semiconductor quantum wells. Raman selection rules and scattering configurations for the observation of the spin-flip transitions in the magneto-Raman scattering are achieved. Our results reveal an unambiguous relation between the conduction band structure and the Raman-scattering spectrum in narrow-gap semiconductor quantum wells. The electron cyclotron mass and the effective Landé  $g$  factor can be directly determined from the dependence of the magneto-Raman spectrum on the filling factor in the Faraday and the Voigt configurations, respectively.

DOI: 10.1103/PhysRevB.66.155303

PACS number(s): 78.30.Fs, 73.21.-b, 71.45.Gm

## I. INTRODUCTION

In recent years we have witnessed a growing interest in spin-related phenomena in low-dimensional semiconductor structures encouraged by their potential application to spin-control devices.<sup>1-3</sup> This interest has been accompanied by an intensive theoretical and experimental study of spin-related properties of low-dimensional systems. Among them, narrow-gap semiconductor-based heterostructures have received a particular attention.

Despite the great advances reached in understanding the properties of narrow-gap heterostructures, many open questions deserve an accurate analysis. In these systems, the combined effects of strong interband coupling, resulting from a narrow gap, lack of inversion symmetry, spatial confinement, as well as the Landau quantization in magnetic fields, lead to a complex interaction between the conduction and valence bands and, consequently, to the relaxation of the optical selection rules. The relevance of the band structure in the simulation of the electronic response related to spin excitations has been stressed by many authors.<sup>3-5</sup> Moreover, interesting features have been recently reported concerning electronic and optical properties of narrow-gap semiconductor quantum wells (QW's) which directly result from their peculiar band structures.<sup>6-8</sup> Standard theories applied to wide-gap structures based on the parabolic band approximation are usually enough to describe the collective response observed in inelastic light-scattering processes.<sup>9,10</sup> However, the physical properties related to the complex electronic band structures are clearly underestimated in the description of several electronic Raman-scattering (ERS) processes such as the spin-flip effect.

Raman scattering appears as a leading tool in the study of

electronic excitations and spin-related phenomena. In the present work we study the effects of the strong interband and intraband admixture on quasi-two-dimensional electron gas in narrow-gap semiconductor QW's in magnetic fields. We show an accurate description of the anisotropic response of the system to external fields, illustrated through the calculations of the ERS spectra. Our theoretical framework is based on the Kane-Weiler  $8 \times 8$   $\mathbf{k} \cdot \mathbf{p}$  Hamiltonian model, and is applied to  $\text{Hg}_{1-x}\text{Cd}_x\text{Te}/\text{CdTe}$  heterostructures. The qualitative achievements of this work can be extended to other zincblende structures in spite of the magnitude of their effective energy gap. The choice of a narrow-gap system was mainly based on its enhanced inter-band coupling on which the discussion is focused.

As long as one considers linear terms in the  $8 \times 8$  Hamiltonian model the coupling of states with different spatial parity and different spin orientation becomes effective. Neglecting warping terms the wave function space can be separated into two orthogonal subspaces<sup>11</sup>

$$|\psi_I\rangle = |k_y\rangle \begin{pmatrix} |f_1^{even}\rangle |N-1\rangle |e\uparrow\rangle \\ |f_2^{even}\rangle |N-2\rangle |hh\uparrow\rangle \\ |f_3^{odd}\rangle |N-1\rangle |lh\downarrow\rangle \\ |f_4^{odd}\rangle |N-1\rangle |so\downarrow\rangle \\ |f_5^{odd}\rangle |N\rangle |e\downarrow\rangle \\ |f_6^{odd}\rangle |N+1\rangle |hh\downarrow\rangle \\ |f_7^{even}\rangle |N\rangle |lh\uparrow\rangle \\ |f_8^{even}\rangle |N\rangle |so\uparrow\rangle \end{pmatrix},$$

$$|\psi_{II}\rangle = |k_y\rangle \begin{pmatrix} |f_1^{odd}\rangle |N-1\rangle |e\uparrow\rangle \\ |f_2^{odd}\rangle |N-2\rangle |hh\uparrow\rangle \\ |f_3^{even}\rangle |N-1\rangle |lh\downarrow\rangle \\ |f_4^{even}\rangle |N-1\rangle |so\downarrow\rangle \\ |f_5^{even}\rangle |N\rangle |e\downarrow\rangle \\ |f_6^{even}\rangle |N+1\rangle |hh\downarrow\rangle \\ |f_7^{odd}\rangle |N\rangle |lh\uparrow\rangle \\ |f_8^{odd}\rangle |N\rangle |so\uparrow\rangle \end{pmatrix}, \quad (1)$$

where  $\psi_I$  and  $\psi_{II}$  label the corresponding carrier ( $e^\pm, hh^\pm, lh^\pm, so^\pm$ ) within a certain QW subband  $m$  and Landau level  $N$ . Warping terms can be included in this formalism as a perturbation, although in the range of fields under consideration their effect can be completely disregarded. The parity of the functions  $f_i^{even(odd)}$  is determined in the growth direction  $z$  with respect to the center of the QW. Thus, conduction band spin states will be represented as  $|e^\pm(N, m)\rangle$ , where the  $+$  and  $-$  states are for the main spin orientation ( $\uparrow$  and  $\downarrow$ ) at the limit of zero magnetic field.

In the case of narrow-gap structures, the coupling of states with different spin orientation is strongly enhanced by the proximity of the conduction and valence bands. The interband coupling induces indirectly an intraband mixing of the conduction spin levels. The electronic states can be approximately described as a linear combination of the different spatial parity functions  $f_i^{even}$  and  $f_i^{odd}$  and the spinors  $|e\uparrow\rangle$  and  $|e\downarrow\rangle$ . In the first conduction subband with  $m=1$  the spin-split states with the same Landau level  $N$  can be described approximately by the wave functions

$$|e^+(N, 1)\rangle \approx f_1^{even}|N\rangle|e\uparrow\rangle + f_5^{odd}|N+1\rangle|e\downarrow\rangle \quad \in \text{subspace I}, \quad (2)$$

$$|e^-(N, 1)\rangle \approx f_1^{odd}|N-1\rangle|e\uparrow\rangle + f_5^{even}|N\rangle|e\downarrow\rangle \quad \in \text{subspace II}. \quad (3)$$

In the following the subband index  $m=1$  will be dropped since we study transitions in the first conduction subband. Notice that we have renumbered the Landau level index of the state  $|e^+(N)\rangle$  as to begin from  $N=0$ . Both states (2) and (3) belonging to the first subband have prominent even components  $f_1^{even}$  and  $f_5^{even}$ , respectively, which are shown in Fig. 1 as a function of magnetic field. The intersubband coupling of states with different spatial parity induces a strong interference, leading to relaxation of the spin-selection rules ( $\Delta S=0$ ). Notice, in Fig. 1, that the components with even parity of both  $|e^+(N)\rangle$  and  $|e^-(N)\rangle$  states are strong at low fields. At high fields, however, the influence of components with odd parity is considerably strong, leading to the mixing of spinors of different spin orientation. This effect, induced by the intersubband coupling, is tuned by the proximity of states of different conduction subbands.

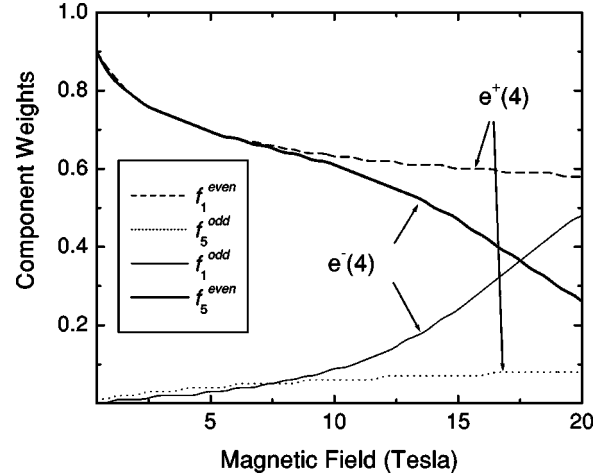


FIG. 1. Component weight dependence on the magnetic field for the spin-split states of the first conduction subband and  $N=4$  for a  $\text{Hg}_{1-x}\text{Cd}_x\text{Te}/\text{CdTe}$  ( $x=0.2$ ) QW of width 100 Å. In the calculation the parameters of Ref. 7 were used.

## II. RAMAN-SCATTERING CROSS SECTION

Magneto-Raman configurations allow for the selective activation of single-particle (in the Faraday configuration) or collective density excitations (in the Voigt configuration). The nature of these excitations is strongly dependent on the Landau level filling factor and the scattering geometry. The angular dependence of the scattering process with respect to the external applied magnetic field  $B_0$  enables us to achieve conditions to study spin-flip Raman scattering, electronic anisotropic effects, and plasma oscillations of a quasi-two-dimensional electron gas. The calculation of the Raman-scattering cross section in the non resonant regime ( $\hbar\omega_L < E_g, \omega_L$  being the frequency of the incident light and  $E_g$  the effective energy gap) is based on the study of the dielectric response of the narrow-gap QW's in magnetic fields.<sup>12,13</sup> The differential scattering cross section for an inelastic scattering process is proportional to the dynamic structure factor given in terms of the response function  $\chi_\alpha(\mathbf{q}, \omega)$ ,

$$\frac{\partial^2 \sigma}{\partial \Omega \partial \omega} \propto \left( \frac{\omega_S}{\omega_L} \right)^2 \text{Im}\{\chi_\alpha(\mathbf{q}, \omega)\}, \quad (4)$$

where  $\omega_S$  is the frequency of the scattered light,  $\omega = \omega_L - \omega_S$  the Raman shift, and  $\mathbf{q} = \mathbf{k}_L - \mathbf{k}_S$  the momentum transfer from the incident light to the elementary excitations. The response function of the single-particle excitations (SPE's) is given by the irreducible polarizability of the electron gas,

$$\chi_0(\mathbf{q}, \omega) = \sum_{N', \alpha; N, \beta} \frac{|\langle e^\alpha(N') | e^{i\mathbf{q}\cdot\mathbf{r}} | e^\beta(N) \rangle|^2}{E^\alpha(N') - E^\beta(N) - \hbar\omega} \times [f_0(\alpha, N') - f_0(\beta, N)], \quad (5)$$

where  $\alpha$  and  $\beta$  stand for the spin orientation  $\pm$  and  $f_0(\alpha, N)$  is the Fermi distribution function. In Eq. (5),  $|e^\pm(N)\rangle$  and  $E^\pm(N)$  are the eigenstate and eigenvalue, respectively, of an electron in the  $N$ th Landau level of the first subband, ob-

tained from the  $8 \times 8$  Kane-Weiler Hamiltonian model.<sup>7</sup> In turn, the charge-density response function is given by

$$\chi_D(\mathbf{q}, \omega) = \frac{\chi_0(\mathbf{q}, \omega)}{\epsilon(\mathbf{q}, \omega)}, \quad (6)$$

where  $\epsilon(\mathbf{q}, \omega)$  is the dielectric function. Within the random-phase approximation, it is given by  $\epsilon(\mathbf{q}, \omega) = 1 - (4\pi e^2/Vq^2)\chi_0(\mathbf{q}, \omega)$ .

The above formalism, based on the random-phase approximation, has provided a good description of the Raman line shape<sup>14</sup> and other properties of two-dimensional electron gas.<sup>15</sup> Note that the exchange interaction is not taken into account in the above formalism.<sup>16</sup> This is an important issue when we consider the system in the quantum Hall regime but it is not relevant for our quantitative analysis of the selection rules relaxation of the ERS. Nevertheless, corrections to the mode dispersion induced by the exchange interaction can be included later through the self-energy renormalization of the uncoupled electronic states.<sup>10</sup>

In this formalism the spatial confinement effect is included within the wave functions and eigenenergies. To describe the Raman process, we choose the backscattering geometry so that the total momentum transfer  $q = (\eta/c)(\omega_L + \omega_S)$  from the light to the internal excitation is maximum, where the refractive index  $\eta$  has been taken as  $\eta = 2.7$ .<sup>17</sup> The Landau level filling is characterized by the factor  $\nu = 2\pi\lambda^2 n_{2D}$ , where  $\lambda = \sqrt{\hbar c/eB_0}$  is the magnetic length and  $n_{2D}$  is the two-dimensional density of electrons (for  $B_0 = 10$  T,  $\nu = 1$  corresponds to  $n_{2D} = 2.4 \times 10^{11} \text{ cm}^{-2}$ ).

Due to the strong anisotropy, induced by the spatial confinement and by the magnetic field, the response function of the system is very sensitive to the angle  $\theta$  of the total internal momentum  $\mathbf{q}$  with respect to the growth direction of the sample. The dependence on the angle  $\theta$  is implicit in the values of the longitudinal and transversal components of the total momentum,  $q_{\parallel} = q \cos \theta$  and  $q_{\perp} = q \sin \theta$ . Notice that, despite the common use, we have assigned  $q_{\parallel}$  parallel to the QW growth direction (taken as the  $z$  direction) and labeled the transverse momentum  $q_{\perp}$  perpendicular to the  $z$  direction (parallel to the well interfaces).

An important effect on the inelastic response of a quasi-two-dimensional electron gas is the appearance of spectra associated with spin-dependent or spin-flip transitions. In Fig. 2 we illustrate the spectra due to the SPE and the charge-density excitations (CDE's) for different values of  $\theta$ . The peak position of the CDE's (labeled by  $P_1$ ) is very sensitive to the transverse scattering wave vector  $q_{\perp}$  according to the plasmon dispersion relation, while the peak positions of the SPE is  $\theta$  independent. The double-peak structure,  $B_1$  and  $B_2$  in Fig. 2(b), is exclusively related to the interband and interlevel coupling effects reflecting a spin dependence<sup>6</sup> of the carrier effective mass. Each peak  $B_1$  corresponds to transitions between the states  $|e^+(0)\rangle$  and  $|e^+(1)\rangle$ , while  $B_2$  indicates transitions between  $|e^-(0)\rangle$  and  $|e^-(1)\rangle$ . The relative shift of the position of these two peaks is due to different effective mass renormalization of each spin level, which de-

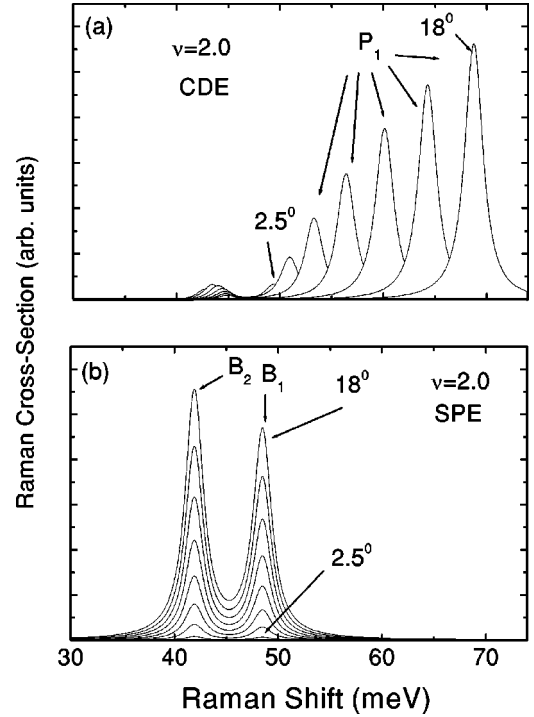


FIG. 2. Electronic magneto-Raman cross section for a  $\text{Hg}_{1-x}\text{Cd}_x\text{Te}/\text{CdTe}$  ( $x=0.2$ ) QW of width  $100 \text{ \AA}$  at  $B_0 = 10$  T and  $\hbar\omega_L = 100$  meV for  $2.5^\circ \leq \theta \leq 18^\circ$ : (a) charge density excitations, (b) single-particle excitations.

pends on the strength of the coupling with higher subbands. This interpretation is supported by the effective mass calculation reported in Ref. 6.

### III. RELAXATION OF THE ERS SELECTION RULES

Two limit cases are pointed as the most relevant ones. The first one is the scattering process shown in Fig. 3(a) for the incoming light along the QW growth direction (the Faraday configuration  $\theta = 0^\circ$ ,  $q_{\parallel} = q$  and  $q_{\perp} = 0$ ). The other one, shown in Figs. 3(b) and 3(c), corresponds to transversal incidence (the Voigt configuration,  $\theta = 90^\circ$ ,  $q_{\perp} = q$  and  $q_{\parallel} = 0$ ). The reason for the selective excitation of different modes lies on the anisotropic electronic structure and the relaxation of intraband transition selection rules due to inter-Landau-level coupling.

Let us analyze in detail the selection rules for intraband transitions. In the case of spin conservation, the transition matrix element is given by

$$\begin{aligned} \langle e^+(N') | e^{i\mathbf{q}\cdot\mathbf{r}} | e^+(N) \rangle &\approx i \langle f_1^{\text{even}}(z) | \cos q_{\parallel} z | f_2^{\text{even}}(z) \rangle \\ &\times \langle N' | e^{iq_{\perp}\rho} | N \rangle \langle e_{\uparrow} | e_{\uparrow} \rangle \\ &+ i \langle f_1^{\text{odd}}(z) | \cos q_{\parallel} z | f_2^{\text{odd}}(z) \rangle \\ &\times \langle N' + 1 | e^{iq_{\perp}\rho} | N + 1 \rangle \langle e_{\downarrow} | e_{\downarrow} \rangle. \end{aligned} \quad (7)$$

The matrix element  $\langle e^-(N') | e^{i\mathbf{q}\cdot\mathbf{r}} | e^-(N) \rangle$  can be obtained analogously.

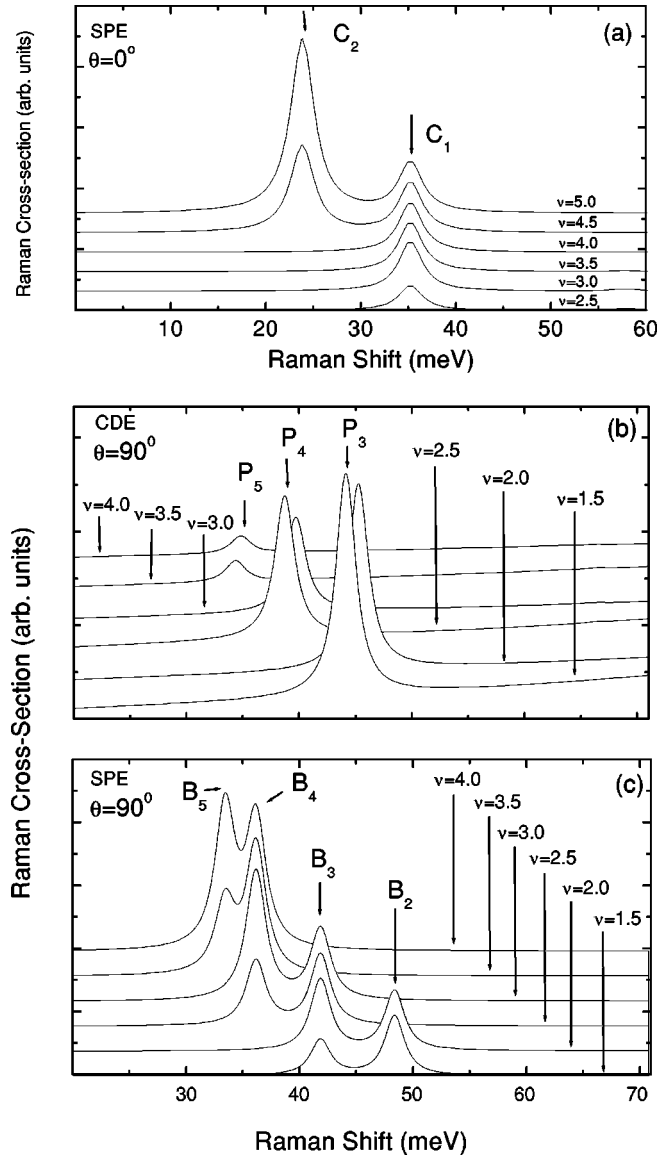


FIG. 3. Electronic magneto-Raman cross section for a  $\text{Hg}_{1-x}\text{Cd}_x\text{Te}/\text{CdTe}(x=0.2)$  QW at  $B_0 = 10$  T,  $\hbar\omega_L = 100$  meV, and different filling factors: (a) for  $\theta = 0^\circ$  (SPE), (b) for  $\theta = 90^\circ$  (CDE), and (c)  $\theta = 90^\circ$  (SPE).

In the framework of a parabolic Hamiltonian model, the electronic transitions induced by the interaction with longitudinal polarization wave must fulfill the spin-selection rule  $\Delta S = 0$ . However, the mixing of components with different spatial parity can induce spin-flip-like transitions between the orthogonal states  $|e^+\rangle$  and  $|e^-\rangle$ . In this case, the corresponding matrix element does not vanish and is given by

$$\begin{aligned}
 \langle e^+(N') | e^{iq_\parallel r} | e^-(N) \rangle &\approx i \langle f_1^{\text{even}}(z) | \sin q_\parallel z | f_2^{\text{odd}}(z) \rangle \\
 &\quad \times \langle N' - 1 | e^{iq_\perp \rho} | N \rangle \langle e^\uparrow | e^\uparrow \rangle \\
 &\quad + i \langle f_1^{\text{odd}}(z) | \sin q_\parallel z | f_2^{\text{even}}(z) \rangle \\
 &\quad \times \langle N' | e^{iq_\perp \rho} | N + 1 \rangle \langle e^\downarrow | e^\downarrow \rangle.
 \end{aligned} \tag{8}$$

Longitudinal interactions represented by Eqs. (7) and (8) are intermediary excitations in Raman-scattering processes.

By analyzing the dependence of the imaginary part of the polarizability on  $Q = \lambda q_\perp / \sqrt{2}$  in the limit  $Q \rightarrow 0$  one can obtain the selection rules corresponding to the configuration with  $\theta \rightarrow 0^\circ$ . In this limit,<sup>7</sup>

$$\begin{aligned}
 \text{Im}\chi_0(\mathbf{q}, \omega) &\propto \langle e^{+(-)}(N') | e^{iq_\parallel r} | e^{-(+)}(N) \rangle \\
 &\propto e^{-Q^2} \sum_{N, N'} (Q^2)^{|N-N'-1|},
 \end{aligned} \tag{9}$$

for the spin-flip transitions, and

$$\begin{aligned}
 \text{Im}\chi_0(\mathbf{q}, \omega) &\propto \langle e^{+(-)}(N') | e^{iq_\parallel r} | e^{+(-)}(N) \rangle \\
 &\propto e^{-Q^2} \sum_{N, N'} (Q^2)^{|N-N'|},
 \end{aligned} \tag{10}$$

for transitions conserving spin.

According to Eq. (9), the inter-Landau-level spin-flip transitions within the first subband ( $\Delta N = N - N' = 1$ ) are allowed in the limit  $Q \rightarrow 0$ . However, the transitions with spin conservation (for which  $\Delta N \neq 0$ ) are forbidden since Eq. (10) results in

$$\lim_{Q \rightarrow 0} [\text{Im}\chi_0(q, \omega)] = 0. \tag{11}$$

Therefore, in the Faraday configuration as  $q_\perp = 0$ , the Raman spectrum describes the SPE with spin-flip transitions only.

Hence, the magneto-Raman spectra in the Faraday configuration ( $\theta \rightarrow 0^\circ$ ) shown in Fig. 3(a) allow for the spin-flip-like inter-Landau-level transitions  $|e^\pm(N)\rangle \rightarrow |e^\mp(N+1)\rangle$  (labeled by  $C_i$ ,  $i = 1$  and  $2$ ), being of a single-particle nature, as indicated by the matrix elements in Eq. (8), while the inter-Landau-level transitions with spin conservation,  $|e^\pm(N)\rangle \rightarrow |e^\pm(N+1)\rangle$ , are forbidden.

For  $\theta > 0^\circ$ , both the SPE and CDE contribute to the cross section but the strongest contributions are related to the inter-Landau-level transitions  $|e^\pm(N)\rangle \rightarrow |e^\pm(N+1)\rangle$ . In the limit  $\theta = 90^\circ$ , these are the uniquely allowed transitions [ $P_i$  and  $B_i$  as shown in Figs. 3(b) and 3(c)]. Each of these peaks corresponds to one excitation mode starting always at one integer value of the filling factor and being effective within a range  $\Delta\nu = 3$ .

According to Eq. (8), the spin-flip intra- [ $|e^\pm(N)\rangle \rightarrow |e^\mp(N)\rangle$ ] and inter-Landau-level transitions  $|e^\pm(N)\rangle \rightarrow |e^\mp(N+1)\rangle$  [see peaks  $C_i$  in Fig. 3(a)] are forbidden in the limit  $\theta = 90^\circ$  since these processes are effective only for finite values of the longitudinal momentum [with  $\sin q_\parallel z \neq 0$ ; see Eq. (8)]. Moreover, the excitation strength dependence on the angle  $\theta$  is directly related to the transverse wave vector modulation of the polarizability function, which makes it also sensitive to the incident light energy.

As a result of the strong intersubband coupling, the electronic properties, such as the effective Landé factor

$$g(N, B_0) = \frac{E^+(N, B_0) - E^-(N, B_0)}{\mu_B B_0}$$

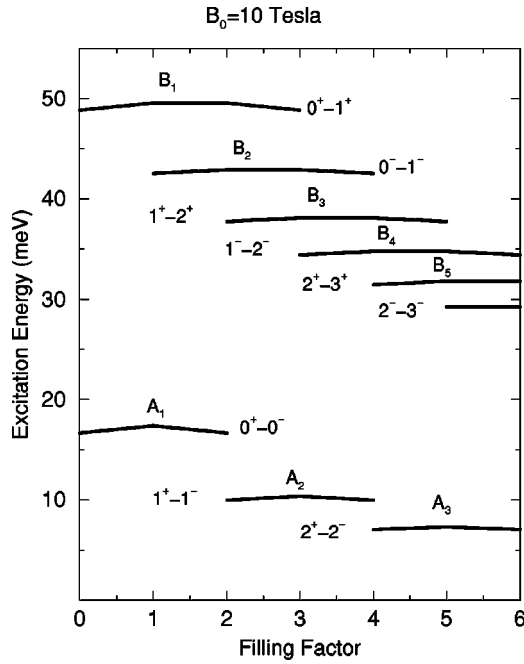


FIG. 4. Excitation stairs as a function of the filling factor  $\nu$  for  $B_0 = 10$  T. The transitions are labeled as  $N^\pm \rightarrow N'^\pm$

and the effective cyclotron mass

$$m_c^\pm(N, B_0) = \frac{\hbar e B_0 / c}{E^\pm(N+1, B_0) - E^\pm(N, B_0)},$$

become strongly dependent on the magnetic field strength  $B_0$ , Landau level index  $N$ , and spin orientation. Such a strong dependence on  $B_0$  and  $\nu$  appears explicitly in the mode dispersion of the SPE as it is described by the response function given by Eq. (5) and shown in Fig. 4. It is important to note that the appearance or not of the excitation peaks in Figs. 3(a) and 3(c) follows the path shown in Fig. 4. Thus, we can assign unambiguously the different SPE peaks, whose position is independent of angle  $\theta$ , to the respective inter- or intra-Landau-level transitions. If we look at the dependence of the excitation energy on the filling factor  $\nu$  in Fig. 4, we find that each mode is active within a certain range of values of  $\nu$ . An analogous analysis can be done for the charge-density excitations for finite values of the angle  $\theta$ .

The modes  $A_i$  in Fig. 4 are related to the intra-Landau-level transitions  $|e^\pm(N)\rangle \rightarrow |e^\mp(N)\rangle$  with spin flip. These modes are active for  $0 < \theta < 90^\circ$  in a range of two consecutive even values of the filling factor  $\nu$  as shown in Fig. 4 with  $\Delta\nu = 2$ . Moreover, the stairlike path is commanded by

the abrupt Landé factor dependence on the Landau level,  $g(N, B_0)$ . In turn, the modes  $B_i$ , induced by the inter-Landau-level excitations with spin conservation, have their path as indicated in Fig. 4. Such a path is dictated by the dependence of the effective mass on the Landau level index and the spin orientation, i.e.,  $m_c^\pm(N, B_0)$ .

The above discussion leads to two important issues: (i) the Landé  $g$  factor can be determined from the Raman-scattering peak position due to the SPE in the Faraday configuration, and (ii) the inverse of the cyclotron mass can be obtained in the Voigt configuration when the plasmon oscillations are switched on. Hence, the Raman spectra due to the SPE and CDE provide us all the necessary information to describe the electronic structure of the conduction subbands in a narrow-gap semiconductor QW.

#### IV. CONCLUSIONS

The principal advantage of a realistic treatment of the complex band structure is that furnishes coherent and comprehensive grounds for the study of the optical properties preventing more complex theoretical models. We have proved that by taking the appropriate interband coupling into account and in the limit case of low transverse momentum or  $\theta \rightarrow 0^\circ$ , the scattering mediated by spin-flip transitions is the leading process. This may help to understand several experimental observations as well as the nature of the spin-flip Raman scattering processes in quasi-two dimensional electron plasmas in the presence of a magnetic field. Another important fact is that the results presented in this work are unambiguously linked to the complex band structure of the narrow-gap systems and can be used to determine their electronic band structure dependence on the Landau level index and magnetic field. It is also shown that integer Landau filling factors can be associated with the limit cases where the picture of the excitation spectrum changes drastically as indicated in Fig. 4 as the result of the interlevel coupling. We have shown that the ERS and the  $8 \times 8$  Kane-Weiler formalism will be very helpful to understand the nature of the optical interlevel transitions, such as the spin-flip ones, and the effects of the interlevel coupling on the energy band shape. The obtained results are a compelling evidence of the interband coupling effects on the nonresonant electronic magneto-Raman scattering in narrow-gap semiconductor QW structures.

#### ACKNOWLEDGMENTS

The authors acknowledge FAPESP and CNPq (Brazil) for financial support.

<sup>1</sup>S.D. Ganichev, E.L. Ivchenko, S.N. Danilov, J. Eroms, W. Wegscheider, D. Weiss, and W. Prettl, Phys. Rev. Lett. **86**, 4358 (2001).

<sup>2</sup>D.P. DiVincenzo, D. Bacon, J. Kempe, G. Burkard, and K.B. Whaley, Nature (London) **408**, 339 (2000).

<sup>3</sup>R.D.R. Bhat and J.E. Sipe, Phys. Rev. Lett. **85**, 5432 (2000).

<sup>4</sup>L. Wissinger, U. Rössler, R. Winkler, B. Jusserand, and D. Rich-

ards, Phys. Rev. B **58**, 15 375 (1998).

<sup>5</sup>A.G. Mal'shukov, K.A. Chao, and M. Willander, Phys. Rev. B **55**, 1918 (1997).

<sup>6</sup>V. López-Richard, G.E. Marques, and C. Trallero-Giner, Solid State Commun. **114**, 649 (2000); **115**, 515(E) (2000).

<sup>7</sup>V. López-Richard, G.E. Marques, and C. Trallero-Giner, J. Appl. Phys. **89**, 6400 (2001).

- <sup>8</sup>C.-M. Hu, J. Nitta, A. Jensen, J.B. Hansen, and H. Takayanagi, *Phys. Rev. B* **63**, 125333 (2001).
- <sup>9</sup>A. Pinczuk, J.P. Valladares, D. Heiman, A.C. Grossard, J.H. English, C.W. Tu, L. Pfeiffer, and K. West, *Phys. Rev. Lett.* **61**, 2701 (1988).
- <sup>10</sup>I.K. Marmorkos and S. Das Sarma, *Phys. Rev. B* **45**, 13 396 (1992).
- <sup>11</sup>V. Lopez-Richard, G. E. Marques, and C. Trallero-Giner, *Physica Status Solidi* **231**, 263 (2002).
- <sup>12</sup>*Light Scattering in Solids IV*, edited by M. Cardona and G. Güntherodt (Springer-Verlag, Berlin, 1984).
- <sup>13</sup>*Elementary Excitations in Solids*, edited by J.D. Jackson and D. Pines (Benjamin, New York, 1964).
- <sup>14</sup>D. Richards, *Phys. Rev. B* **61**, 7517 (2000).
- <sup>15</sup>G. Fasol, N. Mestres, M. Dobers, A. Fisher, and K. Ploog, *Phys. Rev. B* **36**, 1565 (1987).
- <sup>16</sup>A. Pinczuk, B.S. Dennis, D. Heiman, C. Kallin, L. Brey, C. Tejedor, S. Schmitt-Rink, L.N. Pfeiffer, and K.W. West, *Phys. Rev. Lett.* **68**, 3623 (1992).
- <sup>17</sup>*Numerical Data and Functional Relationships in Science and Technology*, edited by O. Madelung, M. Shultz, and H. Weiss, Landolt-Börnsten, New Series, Group III Vol. 17, pt. 3.12.5 (Springer-Verlag, Berlin, 1982).